Sphere anemometer - a faster alternative solution to cup anemometry

M Hölling[1], B Schulte[1], S Barth[2] and J Peinke[1]

[1] ForWind - Center for Wind Energy Research, University of Oldenburg, Germany
[2] ECN Wind Energy, Energy research Centre of the Netherlands

E-mail: michael.hoelling@uni-oldenburg.de

Abstract. We present an anemometer technique characterized by an instrument in a sealed enclosure without moving parts . Measurements taken with our improved sphere anemometer in comparison to cup anemometer and hot-wire anemometer data subjected to wind gusts are discussed. The hot-wire anemometer serves as a reference with high temporal and spacial resolution. A manually driven "gust generator" produced gusts at low frequencies of about $1Hz$. All measurements were carried out in the wind tunnel at the University of Oldenburg.

1. Sphere anemometer - basics

The sphere anemometer uses the relationship between the point force F acting on the tip of a rod and its resulting deflection s.

$$s = \frac{l^3}{3} \cdot \frac{F}{E \cdot J_a}, \tag{1}$$

where l is the length of the rod, E the elasticity modulus and J_a the second moment of area. In case of the sphere anemometer, with a sphere radius r much bigger than the radius of the rod r_R, the force can be assumed to act only on the tip. The second moment of area is then given by

$$J_a = \frac{\pi \cdot r^4}{4} \tag{2}$$

Together with the force acting on the sphere

$$F = \frac{1}{2} \cdot c_d \cdot \rho \cdot A \cdot v^2, \tag{3}$$

where c_d is the drag coefficient of the sphere, A the cross section of the sphere, ρ the density of air and v the wind velocity, equation 1 becomes

$$s = \frac{2}{3} \cdot \frac{l^3 \cdot \rho}{E \cdot r^2} \cdot c_d \cdot v^2 \tag{4}$$

Therefore the deflection of the rod is proportional to the drag coefficient c_d and the wind velocity squared. For a calibration it is necessary to know how

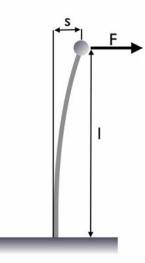**Figure 1.** Bending rod under point force acting on the tip.

the drag coefficient c_d changes with wind velocities. Figure 2 shows the drag coefficient of a sphere plotted against the Reynolds number (Re) (cf [1]). It can be seen that for Reynolds numbers in the range from about 800 to 200000 the change in drag coefficient c_d is negligible. For a sphere with a radius $r = 40mm$ this range in Re corresponds to a range in wind velocities from $0.17m/s$ to $38m/s$ using

$$Re \ = \ \frac{v \cdot 2 \cdot r}{\nu}$$

$$\Rightarrow v \ = \ \frac{Re \cdot \nu}{2 \cdot r},$$

where $\nu = 1.51 \cdot 10^{-5} m^2/s$ is the kinematic viscosity of air. Within this velocity range the deflection s of the rod is directly proportional to the wind velocity squared. With this direct relation it is easy to calibrate the sphere anemometer over a wide range of wind velocities.
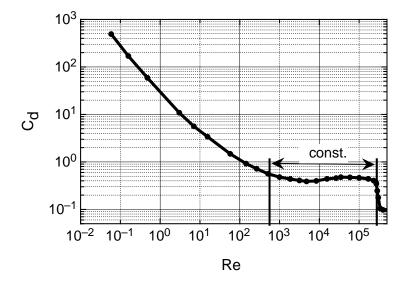

Figure 2. Drag coefficient of a sphere over Reynolds number (cf [1]).

2. Sphere Anemometer - setup

To make use of the relation described in the the last section, we built a sphere anemometer according to figure 3. A sphere with a diameter of $80mm$ is attached to a holder with a much smaller diameter than the diameter of the sphere so the assumption that only the drag of the sphere contributes to the deflection is fulfilled. The holder with the sphere is mounted onto a measuring unit. In this unit the displacement of the sphere and therefore the deflection of the holder is detected. Displacements of the sphere in x- and y-directions are detected simultaneously and converted into voltages. Unlike other sphere anemometers where the displacement is detected by strain gages [2] or proximity sensors [3] we detect the displacement optically using a laser and a **P**osition **S**ensitive **D**etector (PSD) with linear transfer characteristics. A laser beam is focused on a mirror which is attached to the sphere and the reflection hits the PSD located inside the measuring unit. Via calibration, the measured voltages can be related to the horizontal wind speed and direction. The whole setup is adjustable regarding sphere size and material as well as rod length and material. These properties define the resonance frequency of the sphere anemometer which limits the temporal resolution.
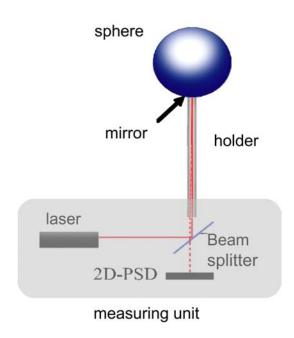
Figure 3. Sketch of sphere anemometer with sphere, holder and measuring unit.

3. Measurements under wind gusts conditions

To investigate the behavior of the sphere anemometer under wind gusts conditions, we designed a manually driven "wind gust generator" (see figure 4, left hand side). A board was brought into the outlet nozzle of the wind tunnel at the University of Oldenburg. This board is attached to a movable axis which can be turned manually. Using this setup we placed three anemometers behind this gust generator; one hot-wire anemometer, one cup anemometer and our sphere anemometer (see figure 4 right hand side).
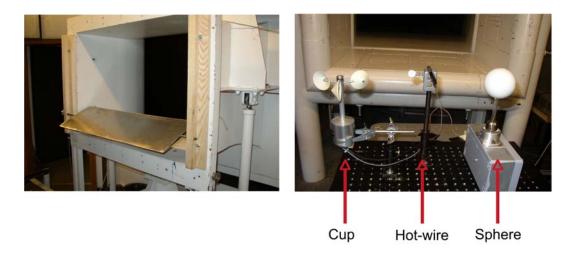

Figure 4. **Left**: Manually driven wind gust generator. **Right**: Position of hot-wire anemometer, cup anemometer and sphere anemometer in the wind tunnel.

All three anemometers were centered at the same hight to make sure they are exposed to the same wind conditions. The hot-wire anemometer was used as a reference, as this anemometer has the highest resolution in time and space to measure the accurate wind velocity. A cup anemometer was used to compare with data acquired with the sphere anemometer. Although the sphere anemometer is capable of measuring the wind velocity in two dimensions, the component only in the main wind direction was measured to compare it with the cup anemometer data.

Figure 5 show the calibration function of the sphere anemometer. It can be seen, that the measured data follows the expected square root function quite well. Using this relation the measured signal can be converted to wind velocities.
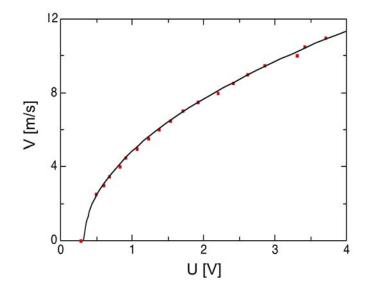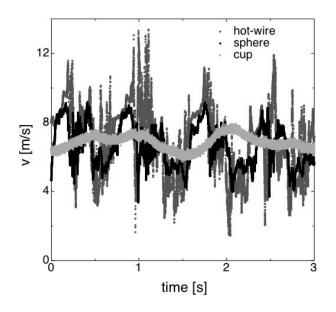

Figure 5. Calibration function of the sphere anemometer. The calibration function follows a square root function.

Figure 6 shows an example of three seconds of the measured velocity of all three anemometers. It can clearly be seen, that the hot-wire anemometer (gray) has the highest temporal resolution and follows even fast extreme changes in the wind velocity. The sphere anemometer (black) however just misses strong changes on small time scales where the cup anemometer cannot resolve the changes in the wind velocity in real time. Due to inertia and over speeding the measured wind gusts are delayed and have a decreased amplitude.

Table 1 shows statistical values measured with all three anemometers. The mean velocity of the hot-wire anemometer and the sphere anemometer are almost the same, the cup anemometer however overestimates the velocity due to over speeding. The standard deviation confirms the statement that the hot-wire has the highest temporal resolution, followed by the sphere anemometer and lastly the cup anemometer. Due to this, all anemometers indicate different turbulence intensities.

Figure 6. Three seconds of measured velocity for all anemometers: hot-wire (gray), sphere (black) and cup (light gray). The cup anemometer cannot follow rapid changes in the wind velocity where the sphere anemometer just misses extreme fast events.

		hot-wire	sphere	cup
mean veolcity	[m/s]	6.3	6.4	6.8
standard dev.	[m/s]	2.2	1.2	0.6
turbulence int.	[%]	34	18	8

Table 1. *Statistical values measured with all three anemometers.*

4. Measurements in the wake of a cylinder

For a more detailed investigation of the temporal resolution we performed measurements in the wake of a cylinder. A cylinder with a diameter of $7cm$ was placed in the wind tunnel with all three anemometers behind it. Figure 7 shows a comparison of the power spectra of data measured with all three anemometers. It can clearly be seen, that the hot-wire anemometer (gray) has the highest response time. It resolves all structures that arise in the flow. It has one peak at the frequency where eddies occur that are caused by the cylinder. The power spectrum of the sphere anemometer (black) shows two peaks. One is caused by the eddies of the Karman street, the other is the natural frequency of the holder which is about $80Hz$. As mentioned before, this natural frequency depends on the selected materials and size of the sphere and the holder. It can clearly be seen that the characteristics of the hot-wire and sphere power spectrum are alike up to the natural frequency of the sphere anemometer. The cup anemometer (light gray) however can not really resolve the structure of the flow. Its response time is too slow so that the cup anemometer more or less just measures the mean wind velocity at all times.
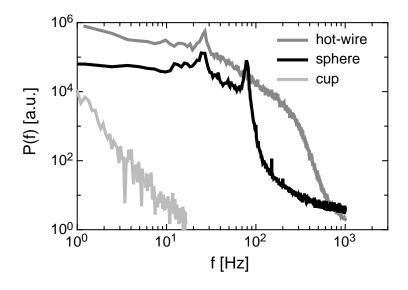
Figure 7. Power spectra of data measured behind a cylinder using hot-wire anemometer (gray), sphere anemometer (black) and cup anemometer (light gray).

5. Conclusions

We presented an improved sphere anemometer which seems to be a promising alternative to cup anemometry. It has no moving parts and therefore no wastage of bearings like the cup anemometer. Wind tunnel experiments under wind gust conditions showed that the sphere anemometer measures the mean wind velocity more accurately than the cup anemometer. Measurements in the wake of a cylinder showed that the response time of the sphere anemometer is much higher than that of the cup anemometer which allows for measurements of atmospheric flows with higher temporal resolution. Such data could be used to predict atmospheric flows on smaller scales or even for a faster regulation of wind turbines.

References

[1] Donley H E 1991 *The Drag Force on a Sphere* (Available at http://www.ma.iup.edu/projects/CalcDEMma/drag/drag.html (21 March 2002))
[2] Wilmer H et al. 1962 *A Simple Fast Response Anemometer* (Journal of Applied Meteorology vol 2 pp 412-416)
[3] Smith S D 1980 *Evaluation of the mark 8 thrust anemometer-thermometer for measurements of boundary-layer turbulence* (Boundary-Layer Meteorology vol 19 pp 273-292)